Lasing without inversion in a four-level diamond system*

Gao Qiang(高 强) and Song Tong-Qiang(宋同强)†

Department of Physics, Ningbo University, Ningbo 315211, *China*

(Received 21 March 2012; revised manuscript received 9 May 2012)

We study the lasing without inversion in a four-level diamond configuration in the case of incoherent pumping field within the framework of the bare-state basis. With the strong fields limit, we obtain the approximate steady-state solution, and discuss the dependence of population distribution and system gain on probe detuning and auxiliary field Rabi frequency.

Keywords: lasing without inversion, four-level diamond system, cyclic transition

PACS: 42.50.Ct, 42.50.Gy **DOI:** 10.1088/1674-1056/21/12/124202

1. Introduction

In the past decades, a large amount of papers have been devoted to the study of light amplification and lasing without the requirement of population inversion (LWI). An attractive idea that is discussed in this context is the possibility to convert a coherent low-frequency input into a coherent high-frequency output by a medium in which no population inversion is realized between atomic levels that generate the high-frequency field. In principle, such a process would lead to coherent amplification in regions of the electromagnetic spectrum where, for various reasons, population inversion is difficult or impossible to achieve. Many models, such as the Λ,[1−5] V,[5−9] Ξ,[5,10−14] quasi-Λ,[15] and N[16] schemes, have been proposed. Various theoretical methods, such as density matrix, master equation,[8−10,12,13,17,18] and the quantum jump[19−21] in the bare and the dressed states, were used. Experimental observations of inversionless gain and lasing without inversion have been reported by several groups.[22−27]

The four-level diamond configuration has been studied theoretically and experimentally in the past. It has been found that the system has some unusual properties related to the phase sensitivity of the process and nonabsorptive states. This configuration also allows the generation of light at telecommunication wavelengths using rubidium and cesium atoms.[28,29] Recently, the experimental investigation of the nondegenerate four-wave mixing[30] and the control of four-level quantum coherence[31] have been reported. In the present paper we study the laser without population inversion in a four-level diamond configuration. By taking the strong coupling field limit, we obtain the approximate steady-state analytical solution of populations and imaginary part of coherences, and discuss the condition for generating laser without inversion, the dependences of population distribution and system gain on Rabi frequency of the auxiliary field and probe detuning. The results show that the auxiliary field is indispensable and must be a strong one in order to present gain. We implement the conversion from lasing without inversion to lasing with inversion by adjusting the system parameters. Due to the coherence and interference effects, the behavior of an excited level population as a function of probe detuning is abnormal: it is at a minimum when resonance, and at a maximum when detuning close to generalized Rabi frequency.

The rest of the present paper is organized as follows. In Sections 2 and 3, we consider the four-level model interacting with three external fields: a weak probe, a strong driving, and a tunable auxiliary one. By taking the strong coupling field limit, we deduce the steady-state analytical solution and the condition for generating laser without inversion. Discussion about the dependence of inversionless gain on system parameters numerically is given in Section 4. Section 5 is devoted to the time-dependent solutions of system populations and coherences for the case of full resonance $\Delta_1 = \Delta_2 = \Delta_3 = 0$. In Section 6 we give the

*Project supported by the K. C. Wong Magna Foundation of Ningbo University, China.

†Corresponding author. E-mail: songtongqiang@nbu.edu.cn

© 2012 Chinese Physical Society and IOP Publishing Ltd

main conclusions and some discussion.

2. Model and equation of motion

Consider a four-level diamond system shown in Fig. 1(a). The transition $|a\rangle \Leftrightarrow |b\rangle$ of frequency ω_{ab} is driven by a strong field of frequency ω_1 with the associated Rabi frequency G_1 and the number of photons N_1. A weak probe field of frequency ω_2 with Rabi frequency G_2 and the number of photons N_2 is applied to the transition between $|a\rangle$ and $|c\rangle$. The corresponding transition frequency is ω_{ac}. The state $|b\rangle$ is driven by an auxiliary field of frequency ω_3 with Rabi frequency G_3 and the number of photons N_3. The corresponding transition frequency between $|b\rangle$ and $|d\rangle$ is ω_{bd}. The transition $|c\rangle \Leftrightarrow |d\,\rangle$ of frequency ω_{cd} is incoherently pumped with the rate Λ. There are spontaneous decays between $|i\rangle$ and $|j\rangle$ described by γ_{ij} $(i,j=a,b,c,d)$. The transitions $|a\rangle \Leftrightarrow |d\,\rangle$ and $|b\rangle \Leftrightarrow |c\rangle$ are dipole forbidden. The auxiliary field is indispensable in our model. If the transition between $|b\rangle$ and $|d\,\rangle$ is driven by an incoherently pumping as shown in Fig. 1(b), instead of the tunable auxiliary field, there is not lasing without inversion at all. This question will be explained in detail in Section 3.

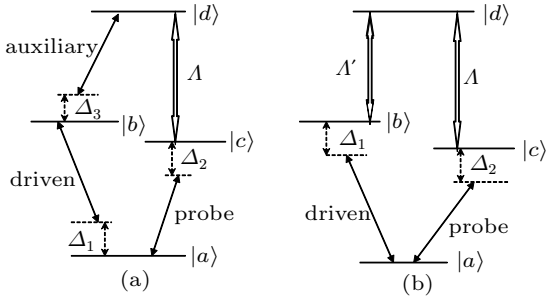


Fig. 1. Four-level diamond models.

The system can be described by the following Hamiltonian in the dipole approximation and rotating-wave approximation:

$$H = H_0 + H_1, \tag{1a}$$

$$H_0 = \hbar\omega_{ab}|b\rangle\langle b| + \hbar\omega_{ac}|c\rangle\langle c| + \hbar\omega_{ad}|d\,\rangle\langle d| + \hbar\omega_1 a_1^\dagger a_1 + \hbar\omega_2 a_2^\dagger a_2 + \hbar\omega_3 a_3^\dagger a_3, \tag{1b}$$

$$H_1 = g_1\big(S_+^{(1)}a_1 + S_-^{(1)}a_1^\dagger\big) + g_2\big(S_+^{(2)}a_2 + S_-^{(2)}a_2^\dagger\big) + g_3\big(S_+^{(3)}a_3 + S_-^{(3)}a_3^\dagger\big), \tag{1c}$$

where H_0 is the unperturbed Hamiltonian of the atom and fields; H_1 is the interaction Hamiltonian between the atom and fields;

$$S_+^{(1)} = |b\rangle\langle a|,\ \ S_+^{(2)} = |c\rangle\langle a|,\ \ S_+^{(3)} = |d\,\rangle\langle b|,$$

and

$$S_-^{(i)} = \big[S_+^{(i)}\big]^*,\ (i=1,2,3)$$

are the raising and lowering operators; g_1, g_2, and g_3 are the coupling constants. Taking the eigenstates of the unperturbed Hamiltonian H_0 as the basis, which are denoted by $|a,N_1+1,N_2+1,N_3+1\rangle$, $|b,N_1,N_2+1,N_3+1\rangle$, $|c,N_1+1,N_2,N_3+1\rangle$, and $|d,N_1,N_2+1,N_3\rangle$, we obtain the matrix form of the total system Hamiltonian as

$$H = \begin{bmatrix} 0 & -\hbar G_1 & -\hbar G_2 & 0 \\ -\hbar G_1 & \hbar\Delta_1 & 0 & -\hbar G_3 \\ -\hbar G_2 & 0 & \hbar\Delta_2 & 0 \\ 0 & -\hbar G_3 & 0 & \hbar(\Delta_1+\Delta_3) \end{bmatrix}, \tag{2}$$

where $-\hbar G_1 = g_1\sqrt{N_1+1}$, $-\hbar G_2 = g_2\sqrt{N_2+1}$, and $-\hbar G_3 = g_3\sqrt{N_3+1}$ are the Rabi frequencies associated with the three coherence fields, respectively; $\Delta_1 = \omega_{ab}-\omega_1$, $\Delta_2 = \omega_{ac}-\omega_2$, and $\Delta_3 = \omega_{bd}-\omega_3$ are the detunings of the external fields. The standard master equation is given by

$$\begin{aligned}\dot\rho = {} & -\frac{\mathrm{i}}{\hbar}[H,\rho] - \frac{\gamma_{ab}}{2}\Big[S_+^{(1)}S_-^{(1)}\rho + \rho S_+^{(1)}S_-^{(1)}\Big] + \gamma_{ab}S_-^{(1)}\rho S_+^{(1)} - \frac{\gamma_{ac}}{2}\Big[S_+^{(2)}S_-^{(2)}\rho + \rho S_+^{(2)}S_-^{(2)}\Big] + \gamma_{ac}S_-^{(2)}\rho S_+^{(2)} \\ & - \frac{\gamma_{bd}}{2}\Big[S_+^{(3)}S_-^{(3)}\rho + \rho S_+^{(3)}S_-^{(3)}\Big] + \gamma_{bd}S_-^{(3)}\rho S_+^{(3)} - \frac{\gamma_{cd}}{2}\Big[S_+^{(4)}S_-^{(4)}\rho + \rho S_+^{(4)}S_-^{(4)}\Big] + \gamma_{cd}S_-^{(4)}\rho S_+^{(4)} \\ & - \frac{\Lambda}{2}\Big[S_+^{(4)}S_-^{(4)}\rho + \rho S_+^{(4)}S_-^{(4)}\Big] + \Lambda S_-^{(4)}\rho S_+^{(4)} - \frac{\Lambda}{2}\Big[S_-^{(4)}S_+^{(4)}\rho + \rho S_-^{(4)}S_+^{(4)}\Big] + \Lambda S_+^{(4)}\rho S_-^{(4)},\end{aligned} \tag{3}$$

where $S_+^{(4)} = |d\,\rangle\langle c|$ and $S_-^{(4)} = |c\rangle\langle d|$ are the raising and lowering operators between state $|c\rangle$ and $|d\,\rangle$ as before. Utilizing master equation (3), we obtain the equation of motion of the density matrix elements as

$$\dot\rho_{aa} = \gamma_{ab}\rho_{bb} + \gamma_{ac}\rho_{cc} + \mathrm{i}G_1(\rho_{ba}-\rho_{ab}) + \mathrm{i}G_2(\rho_{ca}-\rho_{ac}), \tag{4a}$$

$$\dot\rho_{bb} = -\gamma_{ab}\rho_{bb} + \gamma_{bd}\rho_{dd} + \mathrm{i}G_1(\rho_{ab}-\rho_{ba}) + \mathrm{i}G_3(\rho_{db}-\rho_{bd}), \tag{4b}$$

$$\dot\rho_{cc} = -(\gamma_{ac}+\Lambda)\rho_{cc} + (\gamma_{cd}+\Lambda)\rho_{dd} + \mathrm{i}G_2(\rho_{ac}-\rho_{ca}), \tag{4c}$$

$$\dot\rho_{dd} = \Lambda\rho_{cc} - (\gamma_{bd}+\gamma_{cd}+\Lambda)\rho_{dd} + \mathrm{i}G_3(\rho_{bd}-\rho_{db}), \tag{4d}$$

$$\dot{\rho}_{ab} = \mathrm{i}G_1(\rho_{bb}-\rho_{aa}) - \Big(\frac{\gamma_{ab}}{2} - \mathrm{i}\Delta_1\Big)\rho_{ab} + \mathrm{i}G_2\rho_{cb} - \mathrm{i}G_3\rho_{ad}, \tag{4e}$$

$$\dot{\rho}_{ac} = \mathrm{i}G_2(\rho_{cc}-\rho_{aa}) - \Big(\frac{\gamma_{ac}+\Lambda}{2} - \mathrm{i}\Delta_2\Big)\rho_{ac} + \mathrm{i}G_1\rho_{bc}, \tag{4f}$$

$$\dot{\rho}_{ad} = -\mathrm{i}G_3\rho_{ab} - \Big[\frac{\gamma_{bd}+\gamma_{cd}+\Lambda}{2} - \mathrm{i}(\Delta_1+\Delta_3)\Big]\rho_{ad} + \mathrm{i}G_1\rho_{bd} + \mathrm{i}G_2\rho_{cd}, \tag{4g}$$

$$\dot{\rho}_{bc} = -\mathrm{i}G_2\rho_{ba} + \mathrm{i}G_1\rho_{ac} - \Big[\frac{\gamma_{ab}+\gamma_{ac}+\Lambda}{2} + \mathrm{i}(\Delta_1-\Delta_2)\Big]\rho_{bc} + \mathrm{i}G_3\rho_{dc}, \tag{4h}$$

$$\dot{\rho}_{bd} = \mathrm{i}G_3(\rho_{dd}-\rho_{bb}) + \mathrm{i}G_1\rho_{ad} - \Big(\frac{\gamma_{ab}+\gamma_{bd}+\gamma_{cd}+\Lambda}{2} - \mathrm{i}\Delta_3\Big)\rho_{bd}, \tag{4i}$$

$$\dot{\rho}_{cd} = \mathrm{i}G_2\rho_{ad} - \mathrm{i}G_3\rho_{cb} - \Big[\frac{\gamma_{ac}+\gamma_{bd}+\gamma_{cd}+2\Lambda}{2} + \mathrm{i}(\Delta_2-\Delta_1-\Delta_3)\Big]\rho_{cd}. \tag{4j}$$

3. Steady-state analysis on resonance

It is easy to obtain $\mathrm{Re}\,\rho_{ab}^{\mathrm{st}} = \mathrm{Re}\,\rho_{ac}^{\mathrm{st}} = \mathrm{Im}\,\rho_{ad}^{\mathrm{st}} = \mathrm{Im}\,\rho_{bc}^{\mathrm{st}} = \mathrm{Re}\,\rho_{bd}^{\mathrm{st}} = \mathrm{Re}\,\rho_{cd}^{\mathrm{st}} = 0$ by solving the real parts of Eqs. (4e), (4f), (4i), and (4j) and the imaginary parts of Eqs. (4g)–(4h). However even for the exact resonance case ($\Delta_1 = \Delta_2 = \Delta_3 = 0$), it is very complicated to obtain all the steady-state solutions of the set of Eqs. (4a)–(4j). For simplicity, we employ the strong-coupling field approximation, that is, we require $G_1, G_3 \gg G_2, \Lambda$, and γ_{ij} $(i, j \in a, b, c, d)$. Under these conditions, we obtain the populations as

$$\rho_{aa}^{\mathrm{st}} = \frac{G_1^2(\gamma_{bd}+\gamma_{cd}+\Lambda)+G_3^2\gamma_{ab}}{G_1^2(\gamma_{bd}+\gamma_{cd}+\Lambda)}\rho_{bb}^{\mathrm{st}} - \frac{G_1^2\gamma_{ac}+G_3^2\Lambda}{G_1^2(\gamma_{bd}+\gamma_{cd}+\Lambda)}\rho_{cc}^{\mathrm{st}} + \frac{G_3^2(\gamma_{cd}+\Lambda)-G_1^2\gamma_{bd}}{G_1^2(\gamma_{bd}+\gamma_{cd}+\Lambda)}\rho_{dd}^{\mathrm{st}}, \tag{5a}$$

$$\rho_{bb}^{\mathrm{st}} = \frac{G_1^2\gamma_{ac}+G_3^2\Lambda}{G_3^2(\gamma_{ab}+\gamma_{bd}+\gamma_{cd}+\Lambda)}\rho_{cc}^{\mathrm{st}} + \frac{(G_1^2+G_3^2)\gamma_{bd}}{G_3^2(\gamma_{ab}+\gamma_{bd}+\gamma_{cd}+\Lambda)}\rho_{dd}^{\mathrm{st}}, \tag{5b}$$

$$\rho_{cc}^{\mathrm{st}} = \frac{N}{M}\rho_{dd}^{\mathrm{st}}, \tag{5c}$$

$$\rho_{dd}^{\mathrm{st}} = \frac{C}{D}, \tag{5d}$$

where

$$\begin{aligned}
M &= 4G_1^2G_2^2G_3^2(\gamma_{ab}+\gamma_{ac}+\gamma_{bd}+\gamma_{cd}+\Lambda) + G_1^4(\gamma_{ac}+\Lambda)(\gamma_{ab}+\gamma_{bd}+\gamma_{cd}+\Lambda)(\gamma_{ac}+\gamma_{bd}+\gamma_{cd}+2\Lambda)\\
&\quad + 4G_2^2G_3^4\Lambda + G_1^2G_3^2(\gamma_{ac}+\Lambda)^2(\gamma_{ab}+\gamma_{bd}+\gamma_{cd}+\Lambda),\\
N &= 4G_1^2G_2^2G_3^2(\gamma_{ab}+\gamma_{cd}+\Lambda) + G_1^4(\gamma_{cd}+\Lambda)(\gamma_{ab}+\gamma_{bd}+\gamma_{cd}+\Lambda)(\gamma_{ac}+\gamma_{bd}+\gamma_{cd}+2\Lambda)\\
&\quad + 4G_2^2G_3^4(\gamma_{ab}+\gamma_{cd}+\Lambda) + G_1^2G_3^2(\gamma_{ac}+\Lambda)(\gamma_{cd}+\Lambda)(\gamma_{ab}+\gamma_{bd}+\gamma_{cd}+\Lambda),\\
C &= G_1^2G_3^2(\gamma_{ab}+\gamma_{bd}+\gamma_{cd}+\Lambda)\cdot M,\\
D &= (G_1^2+G_3^2)\big[2G_1^2\gamma_{bd} + G_3^2(\gamma_{ab}+\gamma_{cd}+\Lambda)\big]\cdot M + \big[2G_1^4\gamma_{ac} - G_3^4\Lambda + G_1^2G_3^2(\gamma_{ab}-\gamma_{ac}+\gamma_{bd}+\gamma_{cd}+3\Lambda)\big]\cdot N,
\end{aligned}$$

and the probe gain as

$$\begin{aligned}
\mathrm{Im}\,\rho_{ac}^{\mathrm{st}} = \frac{1}{2G_2}\cdot\frac{C}{D\cdot M}\cdot\big[&4G_1^2G_2^2G_3^2(\gamma_{ab}\gamma_{cd}+\gamma_{bd}\gamma_{cd}+\gamma_{cd}^2+\gamma_{cd}\Lambda+\gamma_{bd}\Lambda-\gamma_{ab}\gamma_{ac})\\
&- 4G_2^2G_3^4(\gamma_{ab}\gamma_{ac}+\gamma_{ab}\Lambda+\gamma_{ac}\gamma_{cd}+\gamma_{ac}\Lambda)\big].
\end{aligned} \tag{5e}$$

If the probe field is very weak compared with the spontaneous emission, we ignore all items including G_2 in M and N of Eq. (5c), and obtain $\rho_{cc}^{\mathrm{st}} = (\gamma_{cd}+\Lambda)\rho_{dd}^{\mathrm{st}}/(\gamma_{ac}+\Lambda)$. From Eq. (4c) we know that the steady-state solution is $\mathrm{Im}\,\rho_{ac}^{\mathrm{st}} = -(\gamma_{ac}+\Lambda)\rho_{cc}^{\mathrm{st}}/(2G_2)+(\gamma_{cd}+\Lambda)\rho_{dd}^{\mathrm{st}}/(2G_2)$. This indicates that the probe field does not present gain when it is very weak.

To make the system present gain without inversion, the following conditions need to be satisfied simultaneously:

$$\rho_{aa} - \rho_{cc} > 0, \tag{6a}$$

$$\mathrm{Im}\,\rho_{ac} > 0. \tag{6b}$$

Substituting Eqs. (5a), (5c), and (5e) into Eqs. (6a) and (6b), and taking $G_1 = G_3$, we obtain

$$\begin{aligned}
&(\gamma_{cd}-\gamma_{ac})(\gamma_{ab}+\gamma_{cd}+\Lambda) + \gamma_{bd}(\gamma_{cd}+\Lambda)\\
&\quad - \gamma_{ab}(\gamma_{ac}+\Lambda) > 0,
\end{aligned} \tag{7a}$$

$$4G_2^2(\gamma_{ac}+\gamma_{bd}-\gamma_{ab}-\gamma_{cd}) + (\gamma_{ac}-\gamma_{cd})(\gamma_{ab}+\gamma_{bd}+\gamma_{cd}+\Lambda) \times (2\gamma_{ac}+\gamma_{bd}+\gamma_{cd}+3\Lambda)>0. \quad (7b)$$

On the other hand, the Hamiltonian and equation of motion of the configuration as shown in Fig. 1(b) are presented in the appendix. We can obtain the relation between steady-state system gain and population difference under the condition of the strong-coupling field limit $G_1 \gg G_2$, Λ, Λ', and γ_{ij} as follows:

$$\Big[\frac{2G_1^2(\gamma_{ab}+\Lambda')}{4G_2^2+(\gamma_{ab}+\Lambda')(\gamma_{ab}+\gamma_{ac}+\Lambda'+\Lambda)} + \frac{\gamma_{ac}+\Lambda}{2}\Big]\mathrm{Im}\,\rho_{ac}=G_2(\rho_{cc}-\rho_{aa}). \quad (8)$$

It is clear that the population difference $(\rho_{cc}-\rho_{aa})$ is positive when the system presents gain ($\mathrm{Im}\,\rho_{ac}>0$). This means that only lasing with inversion occurs. Lasing without inversion could not be achieved. Therefore, the auxiliary field is indispensable.

4. Steady-state numerical simulation

In this section, we solve the set of Eqs. (4a)–(4j) in a steady-state regime numerically. We first explore the behavior of population difference and coherences each as a function of the auxiliary field Rabi frequency under resonance condition. Then, we discuss the dependence of inversionless gain on the probe detuning.

The amplification behavior of the probe field can be described by $\mathrm{Im}\,\rho_{ac}$. As plotted in Fig. 2(a), the gain at resonance can be established with the parameters selected appropriately. It can be seen that all the curves start from the negative values. This means that the system displays loss if the auxiliary field is weak. The gain takes the maximum when G_3 is slightly less than G_1. Specifically, the optimal auxiliary field Rabi frequencies for obtaining the gains are $G_3=14.447\gamma_{ac}$, $19.22\gamma_{ac}$, $24\gamma_{ac}$, and $28.783\gamma_{ac}$ corresponding to the value of $G_1=15\gamma_{ac}$, $20\gamma_{ac}$, $25\gamma_{ac}$, and $30\gamma_{ac}$, respectively. The maximum of the gain changes little and the range of G_3 for obtaining gain becomes wider as G_1 increases.

Figure 2(b) shows the variations of steady-state population difference $\rho_{cc}-\rho_{aa}$ with G_3. For not too large G_1, such as $G_1=15\gamma_{ac}$, the system is always in the state without population inversion. For larger values of G_1 (curves for $G_1=20\gamma_{ac}$, $25\gamma_{ac}$, and $30\gamma_{ac}$), the system population distribution may produce population inversion as G_3 increases. Figure 2(c) shows the conversions from lasing without inversion to lasing with inversion. It can be seen that the value of G_3 at which the conversion occurs is always bigger than G_1.

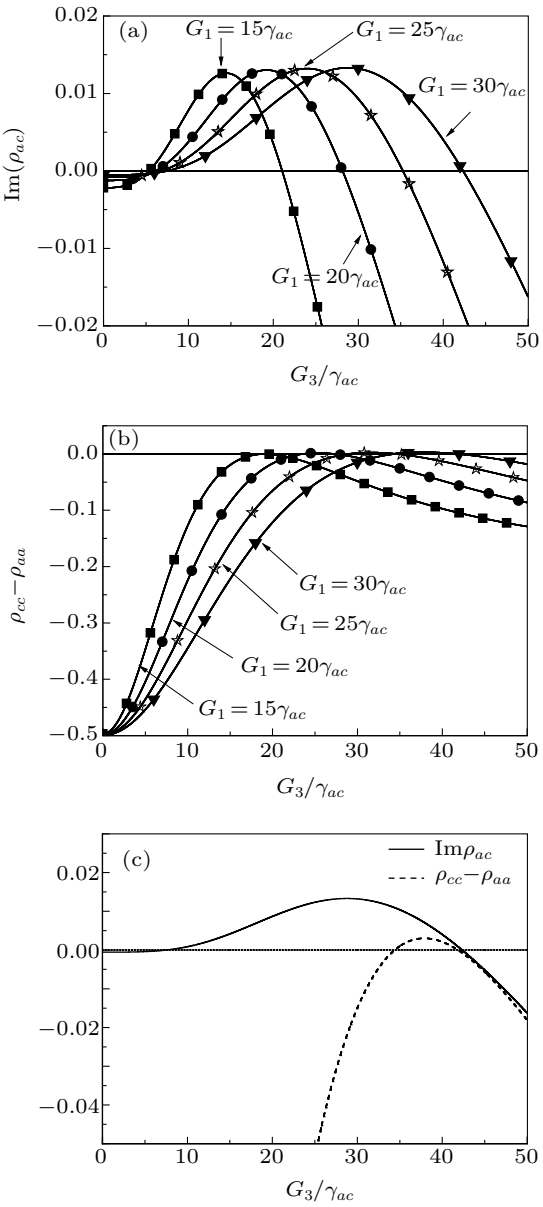


Fig. 2. Steady populations and coherence at resonance for the driven field Rabi frequency $G_1=15\gamma_{ac}$ (square), $20\gamma_{ac}$ (circle), $25\gamma_{ac}$ (pentagon), $30\gamma_{ac}$ (triangle). (a) Steady-state imaginary parts of ρ_{ac} each as a function of the dimensionless parameter G_3/γ_{ac}. (b) Values of steady-state population difference $\rho_{cc}-\rho_{aa}$ each as a function of G_3/γ_{ac}. (c) $\mathrm{Im}\,\rho_{ac}$ (solid line) and $\rho_{cc}-\rho_{aa}$ (dashed line) each as a function of G_3/γ_{ac} for $G_1=30\gamma_{ac}$. The other parameters are $\Delta_1=\Delta_2=\Delta_3=0$, $\gamma_{ab}=\gamma_{ac}=\gamma_{cd}=\Lambda=G_2$, and $\gamma_{bd}=3\gamma_{ac}$.

It can be seen from Fig. 3(a) that an apparent gain can be established under the condition of resonance. The values of gain accord perfectly with our

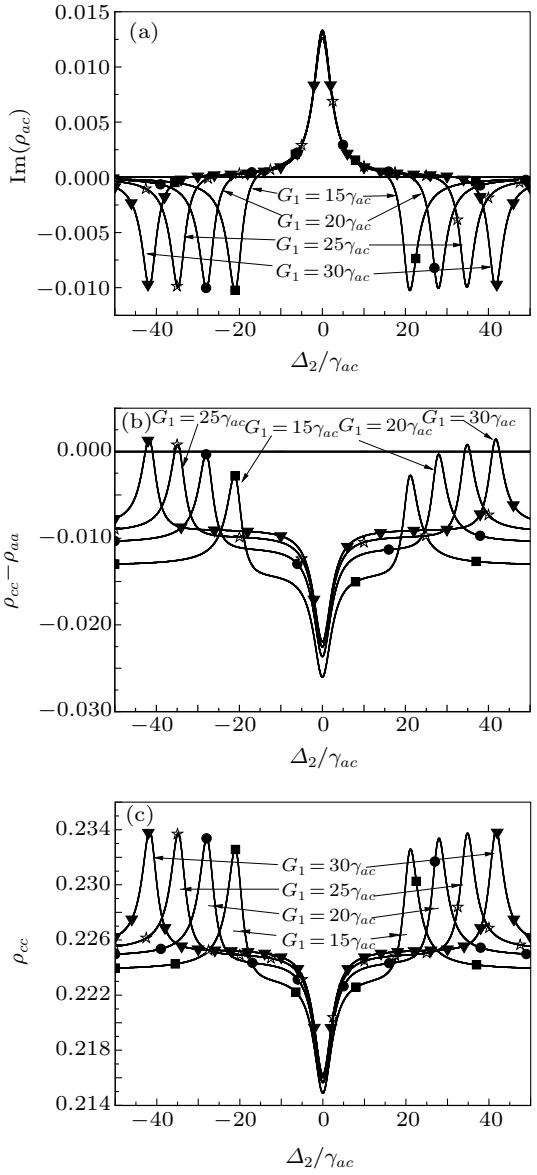


Fig. 3. Steady populations and coherences for the driven field Rabi frequency $G_1 = 15\gamma_{ac}$ (square), $20\gamma_{ac}$ (circle), $25\gamma_{ac}$ (pentagon), $30\gamma_{ac}$ (triangle), showing (a) imaginary parts of ρ_{ac} each as a function of the dimensionless parameter Δ_2/γ_{ac}, (b) values of population difference $\rho_{cc} - \rho_{aa}$ each as a function of Δ_2/γ_{ac}, and (c) an excited level population ρ_{cc} as a function of Δ_2/γ_{ac}. The other parameters are: $\gamma_{ab} = \gamma_{ac} = \gamma_{cd} = \Lambda = G_2$, $\gamma_{bd} = 3\gamma_{ac}$, $\Delta_1 = \Delta_3 = 0$.

analytic prediction of Eq. (5e). The gain reaches its maximum when $\Delta_2 = 0$, and decreases rapidly as absolute value of Δ_2 increases. The range of the gain becomes wider with the value of G_1 increasing. Under the condition of $\Delta_2 = \pm R$, where R is the generalized Rabi frequency defined as $R = \sqrt{G_1^2 + G_2^2 + G_3^2}$, the curves drop to the lowest points. This means that the system presents the most serious loss. Simultaneously, population difference reaches a minimum under the resonance condition (see Fig. 3(b)). As Δ_2 approaches to $\pm R$, the population difference increases or even obtains the population inversion.

Figure 3(c) displays the behaviors of an excited level population ρ_{cc} as a function of probe detuning. The minimum of population ρ_{cc} occurs at $\Delta_2 = 0$ and the maximum occurs at $\Delta_2 = \pm R$, which is an unexpected result. This phenomenon originates from the absorption cancellation by atomic coherence and interference effect.

In short, our results show that the system can present optimal gain without inversion for full resonance ($\Delta_1 = \Delta_2 = \Delta_3 = 0$) and some ranges of parameters G_1 and G_3. Moreover, when G_1 and G_3 are much larger than G_2, Λ, and γ_{ij}, the system presents the conversion from lasing without inversion to lasing with inversion. From Figs. 2 and 3, one can see that our approximations selected in analytical calculation of the part of Section 3 are appropriate. After simple calculation, we find that the degree of error between the approximate set (5a)–(5e) and the exact equations (4a)–(4j) is about a few thousandths.

5. Time-dependent solution

In this section, we obtain the time-dependent solutions of system populations and coherences for the case of full resonance $\Delta_1 = \Delta_2 = \Delta_3 = 0$, by solving numerically the equations of motion under the initial conditions $\rho_{aa}(0) = 1$ and $\rho_{ij}(0) = 0$, $(i \neq j)$. It means that at the initial time, all populations reside at ground state and no prior atomic coherence is present in the system.

From Fig. 4(a), one can see that the population of ground state $|a\rangle$ oscillates fiercely and reaches a steady-state value of 0.239. The population of excited state $|c\rangle$ exhibits an oscillatory increasing behavior and reaches a steady-state value of 0.216. The values of populations accord perfectly with our analytic predictions of Eqs. (5a) and (5c). Figures 4(b)–4(d) describe the variations of imaginary parts of ρ_{ab}, ρ_{ac}, and ρ_{bd}, respectively. It is clear that the loci of gain of driven and auxiliary field are very similar. They oscillate and take a loss ultimately. On the contrary, the imaginary part of probe coherence does not display a pure Rabi oscillation. The time duration is much longer than those of the other two coherences.

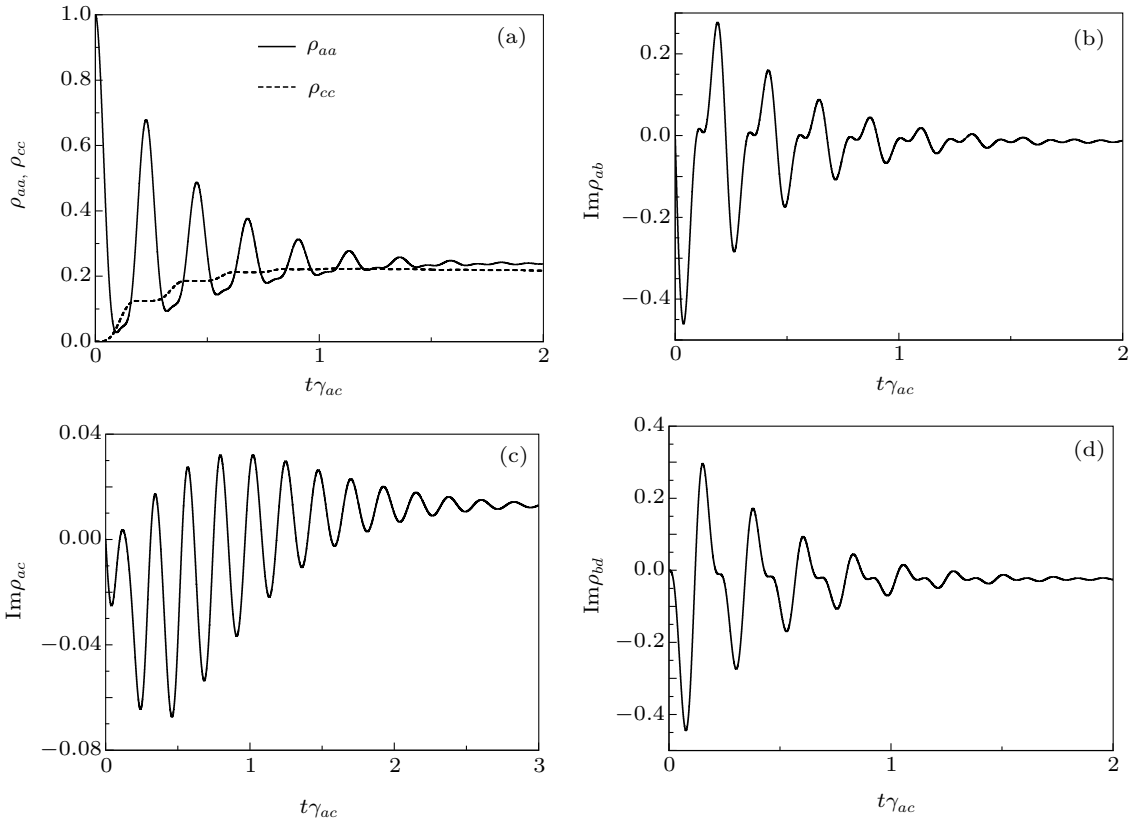


Fig. 4. (a) Population ρ_{aa} (solid line) and ρ_{cc} (dashed line) each as a function of normalized time $t\gamma_{ac}$. (b) Imaginary parts of ρ_{ab} as a function of $t\gamma_{ac}$. (c) Imaginary parts of ρ_{ac} as a function of $t\gamma_{ac}$. (d) Imaginary parts of ρ_{bd} as a function of $t\gamma_{ac}$. The parameters used for the calculation are $G_1 = 20\gamma_{ac}$, $G_2 = \gamma_{ab} = \gamma_{ac} = \gamma_{cd} = \Lambda$, $G_3 = 19.22\gamma_{ac}$, $\gamma_{bd} = 3\gamma_{ac}$, $\Delta_1 = \Delta_2 = \Delta_3 = 0$.

6. Conclusion

We investigated the dynamics of a four-level diamond system interacting with three coherent fields and an incoherent pumping. The gain without inversion of system in a steady-state regime is determined by coherent field Rabi frequency, incoherent pumping rate, and spontaneous emission rate. By using strong coherent field limit, we obtained the approximate steady-state analytical solutions of imaginary part of coherences. The results show that the probe Rabi frequency could not be much smaller than spontaneous emission rate, otherwise there is no probe gain. Particularly, if $\Lambda = \gamma_{ij}$ (incoherent pumping rate and spontaneous emission rates are the same initially) and $G_1 = G_3$ (probe and auxiliary Rabi frequency are equal), the gain of the probe field increases with the increase of spontaneous emission between excited states $|b\rangle$ and $|d\rangle$. It should be pointed out that the coherent auxiliary field plays an important role in this system. To obtain lasing without inversion, the auxiliary field must be strong enough compared with spontaneous emission field. By adjusting the Rabi frequency of the auxiliary field, we can obtain the conversion from lasing without inversion to lasing with inversion.

In this closed loop-transition structure, each level is associated with two transition paths. Due to the coherence and interference effects between the paths, the behavior of an excited level population as a function of probe detuning is abnormal: it is at a minimum when resonance, and at a maximum when detuning closes to the generalized Rabi frequency. Overall, in a four-level diamond configuration, we find a way to achieve gain without inversion. This is instructive for the choice of medium in experiment.

Appendix: Hamiltonian and equation of motion for model shown in Fig. 1(b)

The system Hamiltonian is

$$H = H_0 + H_1, \tag{A1}$$

where

$$H_0 = \hbar\omega_{ab}|b\rangle\langle b| + \hbar\omega_{ac}|c\rangle\langle c| + \hbar\omega_{ad}|d\rangle\langle d| + \hbar\omega_1 a_1^\dagger a_1 + \hbar\omega_2 a_2^\dagger a_2, \quad \text{(A2)}$$

$$H_1 = g_1(S_+^{(1)} a_1 + S_-^{(1)} a_1^\dagger) + g_2(S_+^{(2)} a_2 + S_-^{(2)} a_2^\dagger). \quad \text{(A3)}$$

Here,

$$S_+^{(1)} = |b\rangle\langle a|;\ S_+^{(2)} = |c\rangle\langle a|;\ S_-^{(i)} = [S_+^{(i)}]^\dagger \quad (i = 1, 2)$$

are the raising and lowering operators; g_1 and g_2 are the coupling constants.

Let $\Delta_1 = \omega_{ab} - \omega_1$ and $\Delta_2 = \omega_{ac} - \omega_2$ be the detunings of the external fields, then we will obtain the equation of motion by using master equation as follows:

$$\dot{\rho}_{aa} = \mathrm{i}G_1(\rho_{ba} - \rho_{ab}) + \mathrm{i}G_2(\rho_{ca} - \rho_{ac}) + \gamma_{ab}\rho_{bb} + \gamma_{ac}\rho_{cc}, \quad \text{(A4)}$$

$$\dot{\rho}_{bb} = \mathrm{i}G_1(\rho_{ab} - \rho_{ba}) - (\gamma_{ab} + \Lambda')\rho_{bb} + (\gamma_{bd} + \Lambda')\rho_{dd}, \quad \text{(A5)}$$

$$\dot{\rho}_{cc} = \mathrm{i}G_2(\rho_{ac} - \rho_{ca}) - (\gamma_{ac} + \Lambda)\rho_{cc} + (\gamma_{cd} + \Lambda)\rho_{dd}, \quad \text{(A6)}$$

$$\dot{\rho}_{dd} = \Lambda'\rho_{bb} + \Lambda\rho_{cc} - (\gamma_{bd} + \gamma_{cd} + \Lambda' + \Lambda)\rho_{dd}, \quad \text{(A7)}$$

$$\dot{\rho}_{ab} = \mathrm{i}G_1(\rho_{bb} - \rho_{aa}) - \Big(\frac{\gamma_{ab} + \Lambda'}{2} - \mathrm{i}\Delta_1\Big)\rho_{ab} + \mathrm{i}G_2\rho_{cb}, \quad \text{(A8)}$$

$$\dot{\rho}_{ac} = \mathrm{i}G_2(\rho_{cc} - \rho_{aa}) - \Big(\frac{\gamma_{ac} + \Lambda}{2} - \mathrm{i}\Delta_2\Big)\rho_{ac} + \mathrm{i}G_1\rho_{bc}, \quad \text{(A9)}$$

$$\dot{\rho}_{bc} = -\mathrm{i}G_2\rho_{ba} + \mathrm{i}G_1\rho_{ac} - \Big[\frac{\gamma_{ab} + \gamma_{ac} + \Lambda' + \Lambda}{2} + \mathrm{i}(\Delta_1 - \Delta_2)\Big]\rho_{bc}, \quad \text{(A10)}$$

References

[1] Fan X J, Cui N, Ma H, Li A Y and Li H 2006 *Eur. Phys. J.* D **37** 129

[2] Fan X J, Cui N, Tian S F, Ma H, Gong S Q and Xu Z Z 2005 *J. Mod. Opt.* **52** 2759

[3] Imamoglu A, Field J E and Harris S E 1991 *Phys. Rev. Lett.* **66** 1154

[4] Agarwal G S 1991 *Phys. Rev.* A **44** R28

[5] Kocharovskaya O, Mandel P and Radeonychev Y V 1992 *Phys. Rev.* A **45** 1997

[6] Fan X J, Li J J, Tong D M, Liu C P, Gong S Q and Xu Z Z 2005 *J. Mod. Opt.* **52** 2127

[7] Zhu Y 1992 *Phys. Rev.* A **45** R6149

[8] Hu X M, Xiong J and Peng J S 2001 *Eur. Phys. J.* D **13** 401

[9] Braunstein D and Shuker R 2001 *Phys. Rev.* A **64** 053812

[10] Braunstein D, Koganov G A and Shuker R 2011 *J. Phys.* B: *At. Mol. Opt. Phys.* **44** 235402

[11] Vemuri G, Vasavada K V and Agarwal G S 1995 *Phys. Rev.* A **52** 3228

[12] Braunstein D and Shuker R 2009 *J. Phys.* B: *At. Mol. Opt. Phys.* **42** 125401

[13] Braunstein D and Shuker R 2003 *Phys. Rev.* A **68** 013812

[14] Yang Y L, Liu Z B, Wang L, Tong D M and Fan X J 2009 *Chin. Phys.* B **18** 1054

[15] Liu Z B, Liang Y, Jia K N and Fan X J 2012 *Chin. Phys.* B **21** 024206

[16] Liu Z B, Jia K N, Liang Y, Tong D M and Fan X J 2012 *Chin. Phys.* B **21** 064208

[17] Hu X M and Peng J S 1999 *Eur. Phys. J.* D **5** 291

[18] Hu X M and Peng J S 1998 *J. Phys.* B: *At. Mol. Opt. Phys.* **31** 5393

[19] Claude C, Zambon B and Arimondo E 1993 *J. Opt. Soc. Am.* B **10** 2107

[20] Mompart J and Corbaln R 1998 *Opt. Commun.* **156** 133

[21] Mompart J and Corbaln R 2003 *J. Opt. Soc. Am.* B **20** 2368

[22] Zibrov A S, Lukin M D, Nikonov D E, Hollberg L, Scully M O, Velichansky V L and Robinson H G 1995 *Phys. Rev. Lett.* **75** 1499

[23] Padmabandu G G, Welch G R, Shubin I N, Fry E S, Nikonov D E, Lukin M D and Scully M O 1996 *Phys. Rev. Lett.* **76** 2053

[24] Zhu Y and Lin J 1996 *Phys. Rev.* A **53** 1767

[25] Sellin P B, Wilson G A, Meduri K K and Mossberg T W 1996 *Phys. Rev.* A **54** 2402

[26] Vemuri G, Agarwal G S and Nageswara Rao B D 1996 *Phys. Rev.* A **54** 3695

[27] Kitching J and Hollberg L 1999 *Phys. Rev.* A **59** 4685

[28] Chaneliere T, Matsukevich D N, Jenkins S D, Kennedy T A B, Chapman M S and Kuzmich A 2006 *Phys. Rev. Lett.* **96** 093604

[29] Gomez E, Baumer F, Lange A D, Sprouse G D and Orozco L A 2005 *Phys. Rev.* A **72** 012502

[30] Becerra F E, Willis R T, Rolston S L and Orozco L A 2008 *Phys. Rev.* A **78** 013834

[31] Stowe M C, Peer A and Ye J 2008 *Phys. Rev. Lett.* **100** 203001